Kinetic Approach for Investigating the "Microwave Effect": Decomposition of Aqueous Potassium Persulfate

ARTICLE *in* INDUSTRIAL & ENGINEERING CHEMISTRY RESEARCH · MAY 2011

Impact Factor: 2.59 · DOI: 10.1021/ie200095y

2 AUTHORS:

Basak Temur Ergan
Gebze Technical University
15 PUBLICATIONS **23** CITATIONS
SEE PROFILE

Mahmut Bayramoğlu
Gebze Technical University
83 PUBLICATIONS **2,654** CITATIONS
SEE PROFILE

I&EC research
Industrial & Engineering Chemistry Research

ARTICLE

pubs.acs.org/IECR

Kinetic Approach for Investigating the "Microwave Effect": Decomposition of Aqueous Potassium Persulfate

Başak Temur Ergan* and Mahmut Bayramoğlu

Department of Chemical Engineering, Gebze Institute of Technology, Gebze 41400, Kocaeli, Turkey

Supporting Information

ABSTRACT: In this work, the specific effect of microwave (MW) energy on chemical reactions was investigated by online monitoring of the decomposition kinetics of potassium persulfate ($K_2S_2O_8$). Experiments conducted at constant temperature and constant MW power revealed that the rate constant was about 1.1−1.8 times higher than the rate constant of the thermally heated system at the same temperature, depending on the MW power. To model the dependence of the rate constant on the MW power as $k = f(P)\exp(-g(P)/T)$, various functional forms of MW power were envisaged for $g(P)$ (activation energy E_a) and for $f(P)$ (preexponential factor k_o). Linear, quadratic, and cubic polynomial models were tried for both functions. Nonlinear regression analysis was performed and detailed statistical analysis was applied, and the best results were obtained with quadratic $f(P)$ and cubic $g(P)$ functions, with the highest R^2_{adj} (0.9975) and the lowest standard deviation (0.94×10^{-5}). The mathematical model revealed that both the activation energy and preexponential factor were higher than their thermal counterparts (for $P = 0.75$ kW dm^{-3}, $k_{o,mw}/k_{o,th} = 120$, $E_{a,mw}/E_{a,th} = 1.12$).

1. INTRODUCTION

Today, the use of nontraditional energy sources is being investigated intensively to reduce the processing time and energy consumption and to improve the product quality in process industries. In this respect, microwave (MW) energy is a promising alternative energy source to accelerate chemical and physical phenomena. MW irradiation has several advantages over conventional heating such as instantaneous and rapid bulk heating, selective heating (with materials that can strongly absorb MW in a less polar reaction medium), and energy saving.[1,2]

MW energy is now widely used in various areas of material and food processing industries and has great application potentials in the chemical process industry. The first paper[3] on the use of MW for synthesis reactions appeared in 1986. Today, a huge amount of literature exists on the MW-assisted organic and material synthesis at laboratory scale, which report spectacular improvements that cannot be obtained by conventional heating method.[1−4] These improvements may be summarized as higher yield and selectivity at mild reaction conditions and with shorter reaction times. Furthermore, some reactions that cannot be realized using conventional heating are successfully performed under MW irradiation.[1−4]

According to classical thermodynamics and atomic theory, the energy of a MW photon is too low to break chemical bonds, and in lossy media it can induce only chaotic motions of polar molecules leading to irreversible conversion to thermal energy.[4,5] Meanwhile, outstanding enhancements observed in MW-assisted chemical system results are far from being explained by this classical approach, usually being grouped under the name of "thermal effect" and "nonthermal" or "specific MW effect". Briefly, the thermal effect refers to the acceleration of chemical reaction rates by local temperature rise or the superheating of the medium, while specific effect refers to the rate enhancement by virtue of nonthermal interactions of the medium, including reactant or product molecules with MW photons. Superheating effect reported in the literature is usually explained in the context of "hot-spot" hypothesis successfully applied in sonochemistry.[1,2,6−15] A nonequilibrium thermodynamic approach was also proposed for this purpose.[9−11] On the other side, specific MW effect was claimed by many researchers on the basis of the changes of thermodynamic parameters under MW irradiation.[9−11] The theoretical basis of this hypothesis is still unclear.

It is well-accepted that chemical kinetic study is a strong and comprehensive tool to reveal quantitatively the impact of MW energy on chemical reactions. Various reactions were reported that show similar kinetics in both the presence and absence of MW at comparable temperatures, suggesting the simple dielectric heating of materials by MW.[9−11,16−19] There are reports, however, which show a clear reaction rate enhancement in the presence of MW radiation, indicating a specific MW effect other than the well-accepted dielectric heating.[6−8,20,21] The importance of adequate and accurate temperature control in MW reactor for detecting the MW specific effect by kinetic studies is well-reported.[20−24] It has been proposed that temperature should be measured microscopically due to the temperature gradient in the bulk.[1,11−14,23−27] In recent years, technical developments on temperature, pressure, and power (energy) measurements and process control allowed one to design specialized computer controlled systems that are adapted to chemical synthesis, extending the possibilities of MW-assisted reaction engineering.[20]

In the first comparative kinetic study involving microwave and conventionally heated reactions, Raner et al. demonstrated that

Received: October 28, 2010
Accepted: April 24, 2011
Revised: March 30, 2011
Published: April 24, 2011

nonthermal effects reported by others during the period of 1992−1993 were erroneous.[25,28] Proponents of nonthermal MW effects subsequently altered their hypotheses to account for those results, but the presence of nonthermal effects is still under debate among all of the authors working in MW chemistry.[29] In the kinetic studies, especially after the year 1992, some authors did not find any kinetic difference between Arrhenius parameters (preexponential factor and activation energy) of conventional and MW-assisted reactions.[12,13,30] Contrarily, a great number of articles reported higher preexponential factors[31,32] or lower activation energies[14,26,33−35] in the presence of MW radiation. There are also some papers reporting a different order of reaction and consequently a different reaction mechanism in the presence of MW radiation.[36]

Contradictory experimental results reported in various papers[12−14,26,30−36] may be due to the following reasons:

(a) Applied MW power may not be calculated correctly.

(b) The reaction medium may not be irradiated by constant and continuous MW during the experiment (intermittent or pulsed MW power applications do not fulfill constant MW power condition).

(c) Constant-temperature conditions may not be satisfied properly, especially in isothermal kinetic experiments.

(d) Temperature may not be measured accurately due to the low quality of the temperature sensor or due to the temperature gradients developed in the reaction medium.

(e) The experimental data may not be of sufficient quantity and quality to calculate kinetic parameters accurately.

The aim of this work was to supply reliable kinetic data to elucidate the nature of MW energy−matter interaction in a chemically active system. For this purpose, the radical decomposition kinetics of $K_2S_2O_8$ (an important initiator for free radical polymerization and emulsion polymerization) with simple stoichiometry and simple (first-order) kinetics was chosen

$$\begin{aligned} S_2O_8^{2-} &\rightarrow 2SO_4^{\bullet -} \\ 2SO_4^{\bullet -} + 2e^- &\rightarrow SO_4^{2-} \end{aligned} \quad (1)$$

An interesting study on the MW-assisted decomposition of $K_2S_2O_8$ was conducted by Costa et al.[32] Kinetic experiments were conducted at two different modes; in the constant-temperature experiments, the vials were rapidly heated to the reaction temperature by exposure to high MW irradiation, and after being kept at constant temperature for a certain time interval, they were quenched to stop the reaction. In pulsed irradiation experiments, the samples were repeatedly (1−4 times) heated to 60−90 °C, within short intervals of time (between 24 and 80 s) at high power level and cooled between the heating periods to collect samples for analysis. A gas bulb thermosensor immersed in the reaction medium was used to monitor the reaction temperature. The kinetic parameters were determined for both heating conditions, and no significant differences were found between them, indicating the absence of nonthermal MW effect in this reaction. The authors reported a rate enhancement up to 4 times in comparison with values obtained under conventional heating, which was ascribed to the development of thermal gradients within the sample (the hot spots) arisen from nonhomogeneous distribution of the applied field or from ionic conduction induced by the dissolved sulfate ions.

It must be noted that this study lacks serious drawbacks: First, a limited number of temperatures were investigated and the kinetic calculations were based on a limited number of kinetic data. Furthermore, the experiments were not well organized to assess the effects of temperature and MW power independently. In constant-temperature mode, the MW power were varied from high initial values such as 1200 W to low final values such as 100 W by the control system to maintain the temperature constant. These isothermal experiments are not suitable to reflect the effect of the MW power on the kinetic parameters. On the other hand, the pulsed irradiation experiments were neither conducted at constant temperature nor at constant power conditions. Consequently, the experimental results cannot be used for isothermal kinetic calculations.

In this work, various precautions were undertaken to eliminate various drawbacks of previous kinetic studies. For precise kinetic calculations, an online monitoring system was set up, allowing accurate temperature, concentration, and MW power measurements. The MW power and temperature were selected as primary process variables for the isothermal kinetic plan. MW power was applied continuously to ensure a permanent exposure of the reaction medium to MW irradiation. To accomplish both constant temperature and constant MW power supply during the reaction time, a simple but efficient technique was applied during the reaction by withdrawing thermal energy at a constant rate from the reactor. Finally, mathematical correlations were derived between the kinetic parameters and process variables using an Arrhenius type model. Extensive statistical analysis was conducted to test and validate both the kinetic data and the mathematical models.

2. EXPERIMENTAL SECTION

2.1. Materials. Analytical grade $K_2S_2O_8$ was used directly as received from Merck. Bidistilled water was used in all of the experiments.

2.2. Experimental Setup. The experimental setup is shown in Figure 1. a Pyrex three-necked and round-bottomed glass reactor with 250 cm^3 total volume was used in the experiment. It was insulated with fiberglass and Teflon film to prevent heat loss (insulation thickness, 1.25 cm). The insulation was applied for more precise energy calculations. The materials used in the reactor system were all transparent to MW radiation. For accurate kinetic calculations, uniform conditions of temperature and concentration in the reactor were accomplished by two ways: Magnetic stirring at 160 rpm in the reactor and external circulation of the reaction medium between the reactor and spectrometer flow-through cell at a flow rate between 3 and 35 $cm^3\ min^{-1}$. Furthermore, the flow rate was used also as a control variable to adjust the heat withdrawal rate by cooling the recirculated stream from T_R (the reaction temperature) down to T_C (usually 20 °C, the room temperature) in the cooling bath. Since the liquid flow rate, T_R, and T_C were all constant during the reaction, the heat withdrawal rate was also constant. In this way it was possible to supply continuous MW energy at constant rate to the reaction medium. Precautions were also taken to ensure a well-mixed state in the flow-through cell.

The water samples used in the runs were deoxygenated by purging with N_2 gas prior to the runs. A typical run was accomplished as follows: 10 cm^3 water and 0.8 mmol $K_2S_2O_8$ were loaded into the glass reactor and stirred during 5 min at room temperature for dissolution. Then, 190 cm^3 of distillated water heated to the desired temperature was added rapidly into the reactor and the circulation was started, at the same time N_2 gas was bubbled in the reactor for purging. When the recirculation

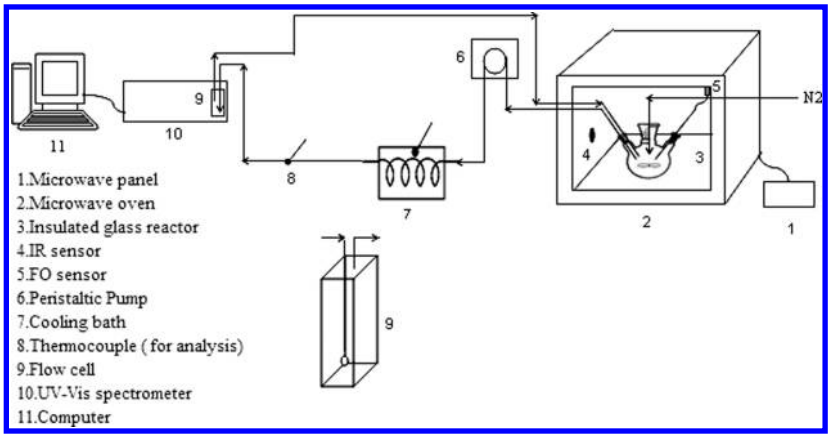

Figure 1. Online MW experimental setup.

line and the flow cell were filled with liquid in approximately 2 min after the addition of hot water, MW energy supply was initiated.

A conventional (thermal) kinetic study was conducted under similar conditions in the same reactor immersed in a water bath (Julabo F-12, Julabo Labortechnik, Seelbach, Germany). The flow rate of the circulated stream was kept constant at 10 cm^3 min^{-1}. The temperatures of the reaction mixture and of the inlet stream to the flow cell were measured by Pt-100 thermocouples (Julabo) with an accuracy of ±0.01 °C.

2.3. Microwave Instrument. In this study, a multimode MW equipment (Start-S model, Milestone S.r.l., Sorisole, Italy) was used, which has the following specifications: cavity volume, 44.73 dm^3; dimensions, 3.5 × 3.3 × 3.7 dm; MW frequency, 2.45 GHz; maximum (nominal) MW power, 1000 W. The control panel of the MW instrument allows setting, controlling, and monitoring various of operational modes such as linear temperature rise, constant temperature, and constant power. On the other hand, magnetic stirring is also provided in situ; for this purpose, a Teflon coated magnet bar is placed in the reactor and the stirring rate is set from the control panel.

For precise temperature measurements, the MW equipment was equipped with two temperature sensors:

(a) A fluoroptic (FO) sensor (ATC-FO-300008 type, MLS GmbH, Leutkirch, Germany) was immersed in the reactor in a glass capillary sheath. The accuracy of the sensor is ±0.2 °C, and the response time is 2 s. This sensor was periodically checked using an instrument (Testo-915-1, Omni Instrument, Dundee, Scotland, U.K.) used for calibration purpose.

(b) An infrared (IR) sensor (accuracy, ±1 °C; IRTC-500 model, Milestone) was used to measure the outer surface temperature of the reactor. As known, the IR sensor's sensitivity is closely related to the distance from the surface of the reactor and surface geometry and color (being transparent or colored).[20] Therefore, in the MW works, the IR sensor was calibrated to monitor the temperature of the insulated surface of the reactor. The surface temperature rise during a run was typically less than 2 °C.

2.4. Calibration of the MW Power Output. The power calibration test was carried out in accordance with the standard method (IEC/EN 60705).[37−39] The details of the calibration procedure and the calculation of MW power P have been described in the Supporting Information. To account for the differences

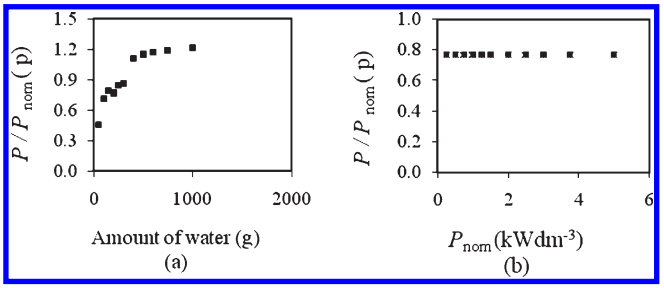

Figure 2. Correction factor (p) as function of (a) water load and (b) P_{nom}.

between the absorbed power P and the applied nominal power P_{nom}, a correction factor (p) was defined as P/P_{nom}. The correction factor versus water load is shown in Figure 2a, and p versus P_{nom} is shown in Figure 2b. According to Figure 2a,b, p is a function of the amount of water but is independent of P_{nom}. p was calculated as 0.768 for the 200 g water load of the reactor used in our experiments.

2.5. Online Monitoring of the Reaction Kinetics. The kinetics of the reaction eq 1 was monitored by measuring online the $K_2S_2O_8$ concentration at 215 nm by spectrophotometric method, which is simpler, faster, and more accurate than the methods used in previous studies.[32,40−45] The calibration procedure and relevant data have been given in detail in the Supporting Information.

2.6. Data Analysis. $K_2S_2O_8$ concentration was held constant in all experiments at 4 mM, which was selected to limit absorbance values under 1.5, as is suggested for spectrophotometric analysis. Reaction conversions were determined according to eq 2, derived from the stoichiometry of the reaction eq 1 and with application of the additivity rule of the molar absorbances of the species in the reaction medium.

$$X_A = 1.02(1 - A/A_0) \quad (2)$$

where the multiplying factor 1.02 is calculated as

$$1/(1 - 2\varepsilon_2/\varepsilon_1) = 1.02 \quad (3)$$

A_0 and A are the absorbances of the reaction medium at the beginning of the reaction and at time t, respectively, X_A is the conversion of $K_2S_2O_8$, and ε_1 and ε_2 are molar absorptivities of

$K_2S_2O_8$ and K_2SO_4, respectively ($\varepsilon_1 = 0.3019\ mM^{-1}\ cm^{-1}$; $\varepsilon_2 = 0.0030\ mM^{-1}\ cm^{-1}$).

On the other hand, the volume of the external line is 3.5 cm^3, and the volume of the flow cell is 3.5 cm^3; thus, the total volume of the reaction mixture outside the MW cavity is 7 cm^3. Because the total reaction medium is 200 cm^3, the reaction volume inside the MW cavity is 193 cm^3. To account for the time spent by the reaction mixture outside the MW oven, the reaction time was calculated as

$$t = (193/200)t_{clock} \quad (4)$$

where t_{clock} is the clock time and t is the reaction time in the system.

2.7. Modeling the Effect of MW Energy on the Rate Constant. For isothermal kinetic experiments, constant temperature must be maintained in the reactor. Furthermore, to discern the specific MW effect, constant power must be supplied to the reaction system. Both constant temperature and constant power conditions seem to be hardly realizable at the same time, since constant (and continuous) power supply results in a nonlinear temperature rise during the reaction. Various isothermal kinetic studies reported in the literature were conducted under intermittent and/or dynamically variable MW power supply,[25,28,32,34,36] which hinders measurement of the effect of the MW power on the rate constant. For a solution of this problem, it was planned to remove a part of the heat content of the reaction medium externally without disturbing the MW field in the cavity of the oven. In this way, it was hoped to supply continuous and constant MW power to the reaction medium.

The experiments showed that the external flow rate (to the flow-through cell of the spectrophotometer) and nominal MW power supply to the oven may be used as process variables which must be set to carefully chosen values to maintain a given MW power constant within 5% error.

In the study, it was planned to investigate the temperature in the range of 70−95 °C and the volumetric MW power in the range of 0.1−0.75 kW dm^3 of reaction volume. These ranges were selected mainly by considering the technical limitations of the MW oven and the reaction system; lower temperature and power values resulted in very long reaction times with noisy kinetic data. On the other hand, it was not possible to reach higher volumetric MW power due to process control problems. It was decided to investigate both parameters at eight levels with an initial plan consisting of 64 experiments. During the course of the study, some experiments at low temperature and at high power density were canceled due to control problems or poor kinetic data, while some auxiliary experiments were included sequentially in the plan at specific points to increase the model quality or to test the error homogeneity. The 86 experiments were presented in detail in Supporting Information Table 2. The mean values of the temperature and volumetric power of each run given in this table were calculated at the end of the run, deviating from the plan (target) values within measurement error.

In conventional heating experiments, the reaction temperature was varied between 58 and 85 °C. Eight conventional experiments were performed under these conditions. The details of the thermal experimental data were given in Supporting Information Table 3.

3. RESULTS AND DISCUSSION

3.1. Estimation of the Experimental Error. To estimate the standard deviation of the experimental rate constant, three replicates were conducted at various process conditions to test also the error homoscedasticity. The results are given in Table 1. To test the homogeneity of variances, Levene's test was applied, which uses the F distribution performing a one-way analysis of variance (ANOVA).[46] According to this test, the probability associated with the F statistic was found to be 0.3864, accepting the variance homogeneity at the 0.05 significance level. Another test used for this purpose is Brown−Forsythe's test[47] according to which the probability associated with the F statistic was calculated as 0.2622, accepting again the assumption of homoscedasticity. In conclusion, the average value of the standard deviation of the experimental error (s) was estimated at 3×10^{-6}.

Table 1. Experimental Error Data

T (°C)	P (kW dm^{-3})	$k \times 10^{-4}$ (s^{-1})	$s \times 10^{-4}$	% relative error
77.2	0.569	0.76	0.03	3.9
86.9	0.684	2.77	0.09	3.2
86.8	0.746	2.60	0.05	1.9
88.4	0.228	3.06	0.07	2.3

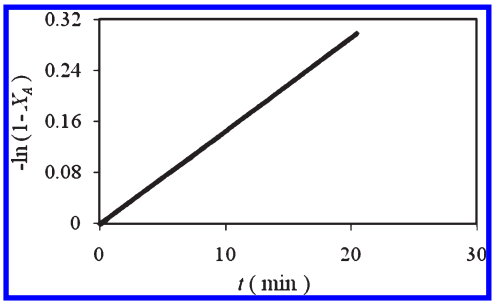

Figure 3. Typical first-order kinetic plot for MW-assisted decomposition of $K_2S_2O_8$. (These experiment conditions are given as no. 5 in Supporting Information Table 2).

3.2. Kinetic Analysis. The kinetic study showed that MW-assisted decomposition kinetics of $K_2S_2O_8$ in aqueous solutions follows first-order rate law similar to the thermal heating mode, as also documented in previous studies.[32,40−45] Excellent fits with correlation coefficient R^2 higher than 0.999 with more than 200 data points were obtained in linear regression for the calculation of the rate constants according to

$$-\ln(1 - X_A) = kt \quad (5)$$

A typical kinetic plot is shown in Figure 3.

The Arrhenius plot related to the thermal heating experiments is shown in Figure 4. The activation energy (E_a) and preexponential factor (k_o) values are given in Table 2. Confidence intervals of 95% for E_a and of $\ln(k_o)$ were estimated as 108.9−121.1 and 31.8636−27.6215, respectively. From the latter interval, the confidence interval for k_o was calculated as $(0.99−68.9) \times 10^{12}$. As seen, both Arrhenius parameters values reported in the literature fall on the lower intervals found in this study. The discrepancies may be due to the low accuracy of their analytical method and limited number of experimental data in the calculation of the kinetic parameters.

3.3. Premodeling Analysis of the Kinetic Data. Experiments showed that the MW power level applied during the reaction influenced the reaction kinetics. The ratio (k_{mw}/k_{th}) is useful to

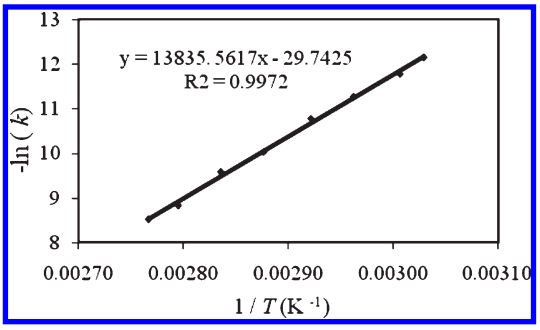

Figure 4. Arrhenius plot of $K_2S_2O_8$ decomposition under thermal heating (thermal experimental data are given in Supporting Information Table 3).

Table 2. Arrhenius Parameters of Thermal Heating

	Arrhenius parameters	
	E_a (kJ mol^{-1})	$k_o \times 10^{12}$ (s^{-1})
this study	115	8.26
Costa[32]	109	1.11

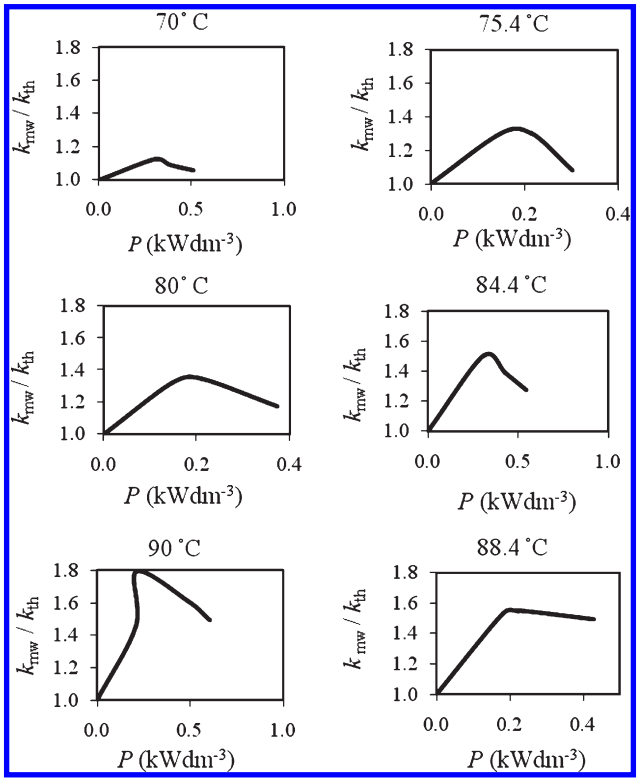

Figure 5. Dependence of the rate constant on MW power at different temperatures.

reflect more clearly the relative impact of MW energy on the reaction kinetics. At low temperatures below 70 °C, this ratio is nearly equal to 1.On the other hand, the highest ratio is 1.8 at the highest temperature investigated in this study (92.3 °C). As also discerned from Figure 5, the functional dependence of the rate constant on the MW power is not as trivial as the Arrhenius law (which reflects the temperature's effect), which is seen

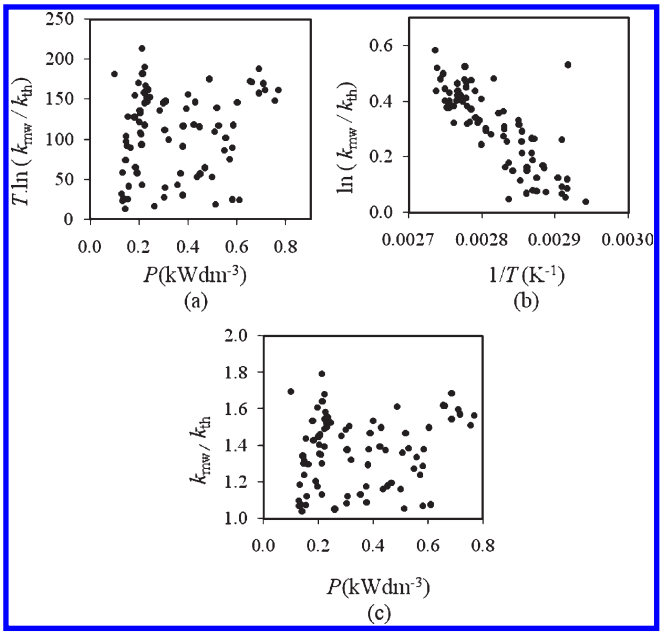

Figure 6. Plots of premodeling analysis of MW data given in Supporting Information Table 2.

also by the dependence of the maximum points on the reaction temperature.

Because no valid theoretical model exists on this subject, a "premodeling" data analysis may be useful to decide on the model type. If an Arrhenius type dependence on temperature is accepted for the rate constant,

$$k_{mw}/k_{th} = (k_{o,mw}/k_{o,th}) \exp[(E_{a,th} - E_{a,mw})/RT] \quad (6)$$

Various cases may be envisaged to check the dependence of the Arrhenius parameters on P. These are outlined as follows.

(1) $k_{o,mw}$ is independent of P and also $k_{o,mw} = k_{o,th}$; then by arranging eq 6

$$T \ln(k_{mw}/k_{th}) = (E_{a,th} - E_{a,mw})/R \quad (7)$$

The plot of $T \ln(k_{mw}/k_{th})$ versus P is given in Figure 6a, which may be used to check the functional dependence of $E_{a,mw}$ on P. A horizontal line is expected for an independence or a well-formed plot for a functional dependence.

(2) $k_{o,mw}$ is independent of P, but $k_{o,mw} \neq k_{o,th}$; then

$$\ln(k_{mw}/k_{th}) = \ln(k_{o,mw}/k_{o,th}) - (E_{a,th} - E_{a,mw})/RT \quad (8)$$

The plot of $\ln(k_{mw}/k_{th})$ versus $1/T$ is given in Figure 6b. A linear plot is expected for the independence of $E_{a,mw}$ from P, in which case $E_{a,mw}$ and $k_{o,mw}$ may be calculated from this (Arrhenius) plot.

Scattered data in Figure 6a,b reject the hypothesis that $k_{o,mw}$ does not depend on P.

(3) $E_{a,mw} = E_{a,th}$ ($E_{a,mw}$ is independent of P); then

$$k_{mw}/k_{th} = k_{o,mw}/k_{o,th} = f(P) \quad (9)$$

k_{mw}/k_{th} is plotted against P in Figure 6c. A well-formed plot is expected for a functional dependence of $k_{o,mw}$ on P. As seen, scattered data are not in favor of the hypothesis that $E_{a,mw}$ is independent of P.

Table 3. Model Types for $f(P)$ and $g(P)$ in Equation 10 [a]

	polynomial degree					$s \times 10^{-5}$		
model no.	$f(P)$	$g(P)$	param no.	R^2_{adj}	R^2_{pred}	s_1	s_2	r
1	linear	quadratic	3	0.9966	0.9965	1.09	1.30	2
2	quadratic	quadratic	4	0.9966	0.9964	1.10	1.33	1
3	**quadratic**	**cubic**	**5**	**0.9975**	**0.9973**	**0.94**	**1.03**	**1**
4	cubic	quadratic	5	0.9973	0.9970	0.97	1.01	1
5	cubic	cubic	6	0.9974	0.9970	0.96	1.05	4

[a] The row in bold indicates the "best" model.

In conclusion, this data analysis leads to the general case that both $k_{o,mw}$ and $E_{a,mw}$ are functions of P.

$$k = f(P)\, e^{[-g(P)/T]} \quad (10)$$

3.4. Mathematical Modeling. The data used for mathematical modeling data have been given in Supporting Information Table 4. In the absence of any theoretical model, various functional forms are envisaged empirically for $f(P)$ and $g(P)$. In this section, the results of a continuing modeling study are presented, where various polynomials are tried for $f(P)$ and $g(P)$. Because the dimension of the kinetic data was large, high-degree polynomials might be tried, but the order was restricted to three for both functions, since preliminary regression studies showed that some higher order models predicted physically impossible kinetic parameters (e.g., negative k_o values).

The nonlinear regression analysis was performed by the Levenberg−Marquardt method[48,49] using the MATLAB optimization toolbox. The standard SSE was minimized as an objective function

$$\mathrm{SSE} = \Sigma e^2 \quad (11)$$

where "e" is the difference between the experimental and model k values (modeling error or residual). The following options was used in the regression: termination tolerance for the objective function, 10^{-20}; maximum function evaluation number, 10^4; maximum iteration number, 10^4. Initially, regression was performed using T (K) as an independent variable. But due to the poor convergence of the minimization task, a variable transformation was found useful from T to $10^3/T$. On the other hand, a logarithmic transformation of the dependent variable (the rate constant) was also attempted in order to improve the results, but generally poor convergence was obtained. Finally, weighted (robust) nonlinear regression analysis was also applied, using another objective function proposed in the literature such as "least median square" or different weight functions. But no improved results were obtained (perhaps due to the homogeneity of the error variance as mentioned in section 3.1).

Various statistics were used for model discrimination. These are, namely, the following: R^2_{adj}, adjusted correlation coefficient which takes into account the number of model parameters; R^2_{pred}, predicted correlation coefficient which reflects the prediction capability of the model; s_1, standard deviation of the residuals; s_2, standard deviation of the studentized residuals; r, number of outliers.

The details of the regression analysis results are given comparatively in Table 3. Some models which did not converge in spite of using various starting points, such as "linear−linear" or "quadratic−linear" models, are not presented in this table.

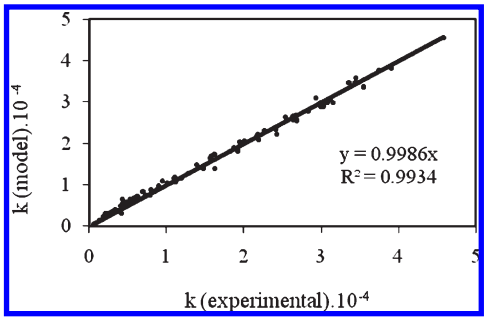

Figure 7. Fit between experimental and model k values for model no. 3.

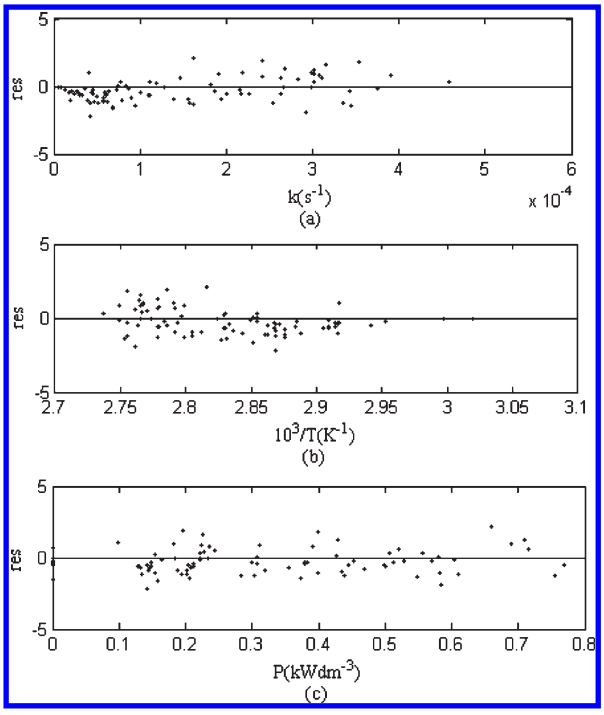

Figure 8. (a) Residual plots between studentized residuals and experimental k, (b) inverse of the temperature, and (c) volumetric MW power.

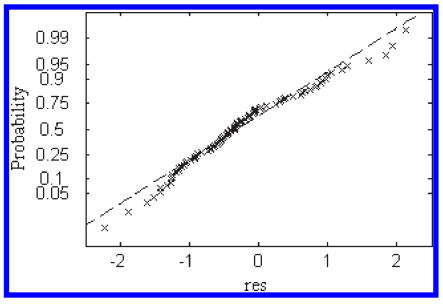

Figure 9. Normal probability plot of the studentized residuals (res).

Table 3 shows that high-order polynomials are necessary to model Arrhenius parameters. This arises probably from the nonlinear (unknown) dependence between P and Arrhenius parameters. All of the criteria presented in Table 3 indicate model no. 3 as the "best" model. In the context of the rule "the simpler the better", model no. 2 may be accepted as the second best model.

dx.doi.org/10.1021/ie200095y |Ind. Eng. Chem. Res. 2011, 50, 6629–6637

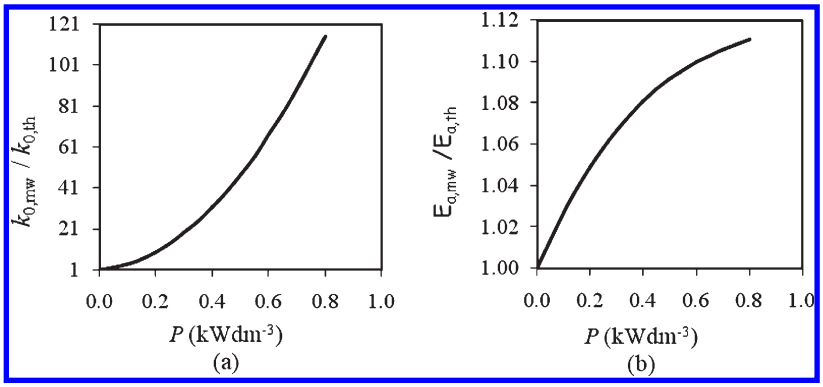

Figure 10. $k_{o,mw}/k_{o,th} - P$ and $E_{a,mw}/E_{a,th} - P$ profile according to model no. 3.

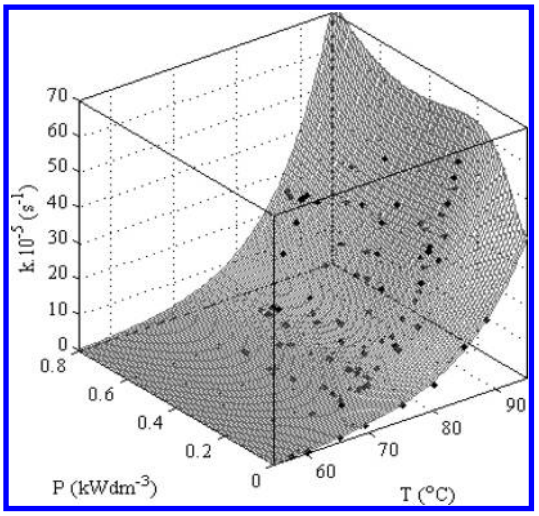

Figure 11. $k - P - T$ surface for model no. 3.

The Arrhenius parameters of model no. 3 are given in

$$k_{o,mw}/s^{-1} = (8.26 + 88P + 1362P^2) \times 10^{12} \quad (12a)$$

$$E_{a,mw}/(\text{kJ mol}^{-1}) = 115.0 + 33.85P - 30.81P^2 + 10.49P^3 \quad (12b)$$

To further test the validity of this model, the fit between experimental and model k values is presented in Figure 7.

On the other hand, a useful tool to test the statistical validity of the model is the residual analysis in order to detect the outliers and test the normality of the residuals. This analysis may be performed graphically; Figure 8 depicts various plots between studentized residuals (res) and the model dependent variable and independent variables. As seen, residual values are randomly distributed and no special trends are detected. Figure 9 presents the normality test of the residuals. In addition to these graphical tests, numerical goodness of fit tests were also performed using the related functions of the MATLAB statistic toolbox such as "Lilliefors test" and "Jarque-Bera test" for model selection and validation purposes.

Model no. 3 was used finally to express graphically the dependence of the kinetic parameters to the volumetric MW power. These are plotted in Figure 10a,b. Surprisingly, the activation energy increases with MW power, up to 12% when compared to the thermal counterpart value for the volumetric MW power value of 0.75 kW dm^{-3}. Furthermore, the 3D surface plot of eqs 12a and 12b for model no. 3 is presented in Figure 11, with experimental data points.

4. CONCLUSION

An experimental setup was designed to investigate the specific (nonthermal) MW effect on the kinetics of chemical reactions. The main characteristics of the systems may be summarized as follows: online monitoring of the reaction extent, which allows getting reliable kinetic data of high number to calculate the rate constant more accurately; online monitoring and control of the reaction temperature using fluoroptic (FO) and IR sensors and online monitoring and control of MW energy supply.

This experimental system allowed setting both the constant temperatures and constant MW energy supply conditions necessary to estimate independently from each other the effects of temperature and MW energy input to a reacting medium, differently from previous kinetic studies.

The experiments showed that MW energy input influences the decomposition rate of $K_2S_2O_8$ in aqueous solution. The reaction order is not affected, but the rate constant is influenced by MW irradiation. The increase in the rate constant is not as high as expected when compared to previously reported values. Thus, these results neither prove nor reject the existence of a strong "specific MW" effect on chemical reactions.

The functional dependence of the rate constant on the MW energy input rate is not as trivial as the Arrhenius law which reflects the temperature's effect. A detailed analysis of the kinetic data revealed that the frequency factor and activation energy are a function of the MW energy supply. Polynomial type functions were used to model the kinetic parameters with temperature and MW energy supply. Nonlinear regression and detailed statistical analysis were performed to validate the model which revealed that both kinetic parameters increase with increasing MW energy supply.

■ ASSOCIATED CONTENT

Supporting Information. Text describing the calibration procedures of the microwave power output and UV, figures showing the load curve for flask containers, UV spectra of $K_2S_2O_8$ and K_2SO_4, calibration curves of $K_2S_2O_8$, and MW-assisted decomposition of $K_2S_2O_8$, and tables listing molar absorptivities, microwave experimental data, thermal (conventional) experimental data, and experimental data for mathematical modeling.

This material is available free of charge via the Internet at http://pubs.acs.org.

AUTHOR INFORMATION

Corresponding Author

*Tel.: 00 90 262 6052113. Fax: 00 90 262 6052105. E-mail: btemur@gyte.edu.tr.

ACKNOWLEDGMENT

We thank the Gebze Institute of Technology (GIT) research fund for partial support.

SYMBOLS

E_a = activation energy (kJ mol^{-1})
k_o = preexponential factor (s^{-1})
T = temperature (°C or K)
T_R = reaction temperature (°C)
T_C = room temperature (usually 20 °C)
k = first-order rate constant (s^{-1})
P = absorbed MW power (or test power) (kW dm^{-3})
P_{nom} = nominal MW power (kW dm^{-3})
p = correction factor for MW power
R^2 = correlation coefficient
s = standard deviation of the experimental error
s_1 = standard deviation of the residuals
s_2 = robust standard deviation of the residuals
t = reaction time or residence time (min)
X_A = Conversion of $K_2S_2O_8$
A = absorbance
r = number of outliers
res = studentized residual

Acronyms

FO = flouroptic sensor
IR = infrared sensor
MW = microwave
SSE = sum of squared errors

Subscripts

mw = MW heating
th = thermal heating (or conventional heating)

REFERENCES

(1) Kappe, C. O. Microwave Dielectric Heating in Synthetic Organic Chemistry. *Chem. Soc. Rev.* **2008**, *37*, 1127.
(2) Clark, D. E.; Folz, D. C.; West, J. K. Processing Materials with Microwave Energy. *Mater. Sci. Eng., A* **2000**, *287*, 153.
(3) Gedye, R.; Smith, F.;The Use of Microwave Ovens for Rapid Organic Synthesis. *Tetrahedron Lett.* **1986**, *27*, 279.
(4) Sanghi, R. Microwave Irradition. Way to Eco-friendly, Green Chemistry. *Resonance* **2000**, 77.
(5) Gabriel, C.; Gabriel, S.; Grant, E. H.; Halstead, B. S. J.; Mingos, D. M. P. Dielectric Parameters Relevant to Microwave Dielectric Heating. *Chem. Soc. Rev.* **1998**, *27*, 213.
(6) Baghurst, D. R.; Mingos, D. M. P. Superheating Effect Associated with Microwave dielectric heating. *J. Chem. Soc., Chem. Commun.* **1992**, 674.
(7) Kuhnert, N. Microwave-Assisted Reactions in Organic Synthesis—Are There Any Nonthermal MW Effects? *Angew. Chem., Int. Ed.* **2002**, *41*, 1863.
(8) Laurent, R.; Laporterie, A.; Dubac, J.; Berlan, J.; Lefeuvre, S.; Audhuy, M. Specific Activation by Microwaves: Myth or Reality? *J. Org. Chem.* **1992**, *57*, 7099.
(9) Perreux, L.; Loupy, A. A Tentative Rationalization of Microwave Effects in Organic Synthesis According to the Reaction Medium, and Mechanistic Considerations. *Tetrahedron* **2001**, *57*, 9199.
(10) De La Hoz, A.; Diaz-Ortiz, A.; Moreno, A. Microwaves in Organic Synthesis. Thermal and Non-thermal Microwave Effects. *Chem. Soc. Rev.* **2005**, *34*, 164.
(11) Perreux, L.; Loupy, A. *Microwaves in Organic Synthesis*; Wiley: Weinheim, Germany, 2002.
(12) Lidstrom, P.; Tierney, J.; Wathey, B.; Westman, J. Microwave Assisted Organic Synthesis—A Review. *Tetrahedron.* **2001**, *57*, 9225.
(13) Berlan, J. Microwaves in Chemistry: Another Way of Heating Reaction Mixtures. *Rad. Phys. Chem.* **1995**, *45*, 581.
(14) Lewis, D. A.; Summers, J. D.; Ward, T. C.; McGrath, J. E. Accelerated Imidization Reactions Using Microwave Radiation. *J. Polym. Sci., Part A: Polym. Chem.* **1992**, *30*, 1647.
(15) Kabza, K. G.; Chapados, B. R.; Gestwicki, J. E.; McGrath, J. L. Microwave-Induced Esterification Using Heterogeneous Acid Catalyst in a Low Dielectric Constant Medium. *J. Org. Chem.* **2000**, *65*, 1210.
(16) Esveld, B.; Chemat, F.; Haveren, J. V. Pilot Scale Continuous Microwave Dry-Media Reactor, Part I: Design and Modeling. *Chem. Eng. Technol.* **2000**, *23*, 3.
(17) Esveld, B.; Chemat, F.; Haveren, J. V. Pilot Scale Continuous Microwave Dry-Media Reactor, Part II: Application to Waxy Esters Productions. *Chem. Eng. Technol.* **2000**, *23*, 5.
(18) Xiaoqing, Y.; Kama, H. Study on the Key Problems of Interaction between Microwave and Chemical Reaction. *Front. Electr. Electron. Eng.* **2007**, *2*, 473.
(19) Herrero, M. A.; Kremsner, J. M.; Kappe, C. O. Nonthermal Microwave Effects Revisited: On the Importance of Internal Temperature Monitoring and Agitation in Microwave Chemistry. *J. Org. Chem.* **2008**, *73*, 36.
(20) Nuchter, M.; Ondruschka, B.; Bonrath, W.; Gum, A. Microwave assisted synthesis—A Critical Technology Overview. *Green Chem.* **2004**, *6*, 128.
(21) Strauss, C. R. Microwave-Assisted Reactions in Organic Synthesis—Are There Any Nonthermal Microwave Effects? Response to the Highlight by N. Kuhnert. *Angew. Chem., Int. Ed.* **2002**, *41*, 3589.
(22) Stadler, A.; Pichler, S.; Horeis, G.; Kappe, C. O. Microwave-Enhanced Reactions under Open and Closed Vessel Conditions. A Case Study. *Tetrahedron* **2002**, *58*, 3177.
(23) Jahngen, E. G. E.; Lentz, R. R.; Pesheck, P. S.; Sackett, P. H. Hydrolysis of Adenosine Triphosphate by Conventional or Microwave Heating. *J. Org. Chem.* **1990**, *10*, 3406.
(24) Hosseini, M.; Stiasni, N.; Barbieri, V.; Kappe, C. O. Microwave-Assisted Asymmetric Organocatalysis: A Probe for Nonthermal Microwave Effects and the Concept of Simultaneous Cooling. *J. Org. Chem.* **2007**, *72*, 1417.
(25) Raner, K. D.; Strauss, C. R.; Vyskoc, F.; Mokbel, L. A Comparison of Reaction Kinetics Observed under Microwave Irradiation and Conventional Heating. *J. Org. Chem.* **1993**, *58*, 950.
(26) Shibata, C.; Kashima, T.; Ohuchi, K. Nonthermal Influence of Microwave Power on Chemical Reactions. *Jpn. J. Appl. Phys.* **1996**, *35A*, 316.
(27) He, W.-D.; Pan, C.-Y.; Lu, T. Soapless Emulsion Polymerization of Butyl Methacrylate through Microwave Heating. *J. Appl. Polym. Sci.* **2001**, *80*, 2455.
(28) Raner, K. D.; Strauss, C. R. Influence of Microwave on the Rate of Esterification of 2,4,6-Trimethylbenzoic Acid with 2-Propanol. *J. Org. Chem.* **1992**, *57*, 6231.
(29) Perreux, L.; Loupy, A. *Microwaves in Organic Synthesis*; Wiley: Weinheim, Germany, 2006.
(30) Galema, S. A. Microwave Chemistry. *Chem. Soc. Rev.* **1997**, *26*, 233.
(31) Binner, J. G. P.; Hassine, N. A.; Cross, T. E. The Possible Role of Pre-exponential Factor in Explaining the Increased Reaction-Rates Observed during the Microwave Synthesis of Titanium Carbide. *J. Mater. Sci.* **1995**, *21*, 5389.
(32) Costa, C.; Santos, V. H. S.; Araujo, P. H. H.; Sayer, C.; Santo, A. F.; Fortuny, M. Microwave-Assisted Rapid Decomposition of Persulfate. *Eur. Polym. J.* **2009**, *45*, 2011.

(33) Bao, J.; Zhang, A. Poly(methyl methacrylate) Nanoparticles Prepared through Microwave Emulsion Polymerization. *J. Appl. Polym. Sci.* **2004**, *93*, 2815.

(34) Adnadevic, B.; Gigov, M.; Sindjic, M.; Jovanovic, J. Comparative Study on Isothermal Kinetics of Fullerol Formation under Conventional and Microwave Heating. *Chem. Eng. J.* **2008**, *140*, 570.

(35) Kuslu, S.; Bayramoglu, M. Microwave-Assisted Dissolution of Pyrite in Acidic Ferric Sulfate Solutions. *Ind. Eng. Chem. Res.* **2002**, *41*, 5145.

(36) Wragg, D. S.; Byrne, P. J.; Giriat, G.; Ouay, B. L.; Gyepes, R.; Harrison, A.; Whittaker, A. G.; Morris, R. E. In Situ Comparison of Isothermal Kinetics under Microwave and Conventional Heating. *J. Phys. Chem.* **2009**, *113*, 20553.

(37) *Household Microwave Ovens—Methods for Measuring Performance*, Standard No. 60705; International Electrotechnical Commission: Geneva, Switzerland,2006

(38) Soltysiak, M.; Erle, U.; Celuch, M. Load Curve Estimation for Microwave Ovens: Experiments and Electromagnetic Modelling. *Mlkon Conf. Proc.* **2008**, *1*, 633.

(39) Swain, M. J.; Ferron, S.; Coelho, A. I. P.; Swain, M. V. L. Effect of Continuous (Intermittent) Use on the Power Output of Domestic Microwave Ovens. *Int. J. Food Sci. Technol.* **2006**, *41*, 652.

(40) Price, G. J.; Clifton, A. A. Sonochemical Acceleration of Persulfate Decomposition. *Polym. Commun.* **1996**, *37*, 3971.

(41) Beylerian, N. M.; Vardanyan, L. R.; Harutyunyan, R. S.; Vardanyan, R. L. Kinetics and Mechanism of Potassium Persulfate Decomposition in Aqueous Solutions Studied by a Gasometric Method. *Macromol. Chem. Phys.* **2002**, *203*, 212.

(42) Santos, A. M.; Vindevoghel, P. H.; Graillat, C.; Guyot, A.; Guillot, J. Study of the Thermal Decomposition of Potassium Persulfate by Potentiometry and Capillary Electrophoresis. *J. Polym. Sci., Part A: Polym. Chem.* **1996**, *34*, 1271.

(43) Li, J.; Zhu, X.; Zhu, J.; Cheng, Z. Microwave-Assisted Nitroxide-Mediated Miniemulsion Polymerization of Styrene. *Radiat. Phys .Chem.* **2007**, *76*, 23.

(44) Zhu, X.; Chen, J.; Cheng, Z.; Lu, J.; Zhu, J. Emulsion Polymerization of Styrene under Pulsed Microwave Irradiation. *J. Appl. Polym. Sci.* **2003**, *89*, 28.

(45) Zhu, X.; Chen, J.; Zhou, N.; Cheng, Z.; Lu, J. Emulsion Polymerization of Methyl Methacrylate under Pulsed Microwave Irradiation. *Eur. Polym. J.* **2003**, *39*, 1187.

(46) Levene, H. Robust Tests for Equality of Variances. *Contributions to Probability and Statistics. Essays in Honor of Harold Hotelling*; Stanford University Press: Palo Alto, CA, 1960.

(47) Brown, M. B.; Forsythe, A. B. Robust Tests for the Equality of Variances. *J. Am. Stat. Assoc.* **1974**, *69*, 364.

(48) Levenberg, K. A Method for the Solution of Certain Non-Linear Problems in Least Squares. *Q. Appl. Math.* **1944**, *2*, 164.

(49) Marquardt, D. An Algorithm for Least-Squares Estimation of Nonlinear Parameters. *SIAM J. Appl. Math.* **1963**, *11*, 431.